Journal of Colloid and Interface Science 566 (2020) 202–210

Contents lists available at ScienceDirect

Journal of Colloid and Interface Science

journal homepage: www.elsevier.com/locate/jcis

Compartmentalization of gold nanoparticle clusters in hollow silica spheres and their assembly induced by an external electric field

Kanako Watanabe [a], Tom A.J. Welling [b], Sina Sadighikia [b], Haruyuki Ishii [c], Arnout Imhof [b], Marijn A. van Huis [b], Alfons van Blaaderen [b], Daisuke Nagao [a,*]

[a] Department of Chemical Engineering, Tohoku University, 6-6-07 Aoba, Aramaki-aza, Aoba-ku, Sendai, Miyagi 980-8579, Japan
[b] Soft Condensed Matter, Debye Institute for Nanomaterials Science, Utrecht University, Princetonplein 5, 3584 CC Utrecht, the Netherlands
[c] Department of Sustainable Environmental Engineering, Yamaguchi University, 2-16-1, Tokiwadai, Ube, Yamaguchi 755-0097, Japan

HIGHLIGHTS

- Mobile gold nanoparticle clusters encapsulated into hollow silica spheres.
- The hollow spheres assembled in a specific space by external electric fields.
- Reversible control over the assembled and dispersed states of the hollow spheres.
- Raman intensities depending on the assembled states of the hollow spheres.
- The hollow spheres providing compartments to keep the clusters colloidally stable.

GRAPHICAL ABSTRACT

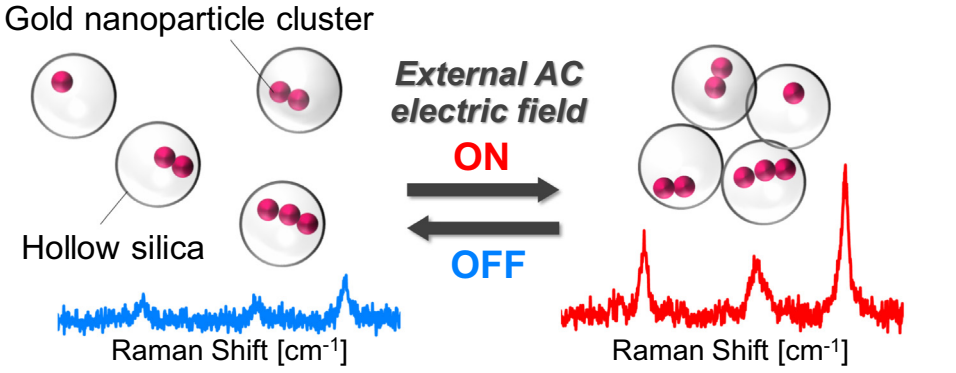

ARTICLE INFO

Article history:
Received 12 December 2019
Revised 17 January 2020
Accepted 24 January 2020
Available online 25 January 2020

Keywords:
Plasmonic nanoparticles
Nanoparticle clusters
Plasmonic properties
surface-enhanced Raman scattering
Hollow particles
Particle assembly

ABSTRACT

Assembly of plasmonic nanoparticle clusters having hotspots in a specific space is an effective way to efficiently utilize their plasmonic properties. In the assembly, however, bulk-like aggregates of the nanoparticles are readily formed by strong van der Waals forces, inducing a decrease of the properties. The present work proposes an advanced method to avoid aggregation of the clusters by encapsulating into a confined space of hollow silica interior. Hollow spheres incorporating gold nanoparticle clusters were synthesized by a surface-protected etching process. The observation of inner nanoparticles with liquid cell transmission electron microscopy experimentally proved that the nanoparticles moved as a cluster instead of as dispersed nanoparticles within the water-filled hollow compartment. The hollow spheres incorporating the nanoparticle clusters were assembled in the vicinity of electrodes by application of an external AC electric field, resulting in the enhancement of Raman intensities of probe molecules. The nanoparticle-cluster-containing hollow spheres were redispersed when the electric field was turned off, showing that the hollow silica spheres can act as a physical barrier to avoid the cluster aggregation. The Raman intensities were reversibly changed by switching the electric field on and off to control the assembled or dispersed states of the hollow spheres.

Abbreviations: Au NPs, gold nanoparticles; LSPR, Localized surface plasmon resonance; SERS, Surface-enhanced Raman scattering; TEOS, tetraethyl orthosilicate; PMBA, 4-mercaptobenzoic acid; NH_3, ammonia aqueous solution; PEI, polyethylenimine; SiO_2, silica; m-Au@SiO_2, silica sphere incorporating multiple gold nanoparticles; m-Au@hSiO_2, hollow silica sphere incorporating multiple gold nanoparticles; LCTEM, liquid cell transmission electron microscopy.

* Corresponding author.
E-mail address: dnagao@tohoku.ac.jp (D. Nagao).

https://doi.org/10.1016/j.jcis.2020.01.094
0021-9797/

1. Introduction

Nanoparticles (NPs) smaller than 100 nm exhibit physical and chemical properties different from those of bulk materials. In particular, noble metal NPs such as silver and gold NPs, which are plasmonic NPs, are well known to exhibit unique properties (e.g. catalytic [1], magnetic [2], optical [3], and sensing properties [4]). A localized surface plasmon resonance (LSPR), in which light of specific wavelengths excites a collective oscillation of conduction band electrons, is a typical phenomenon of these NPs. One application of this, Surface-enhanced Raman scattering (SERS), has received enormous interest since it was discovered in the 1970s [5,6]. Because strong Raman intensities are obtained from molecules neighboring NP surfaces, SERS is a promising phenomenon for developing highly sensitive sensors, particularly targeting biomolecules [7,8]. These properties of plasmonic NPs are explained by the following mechanism: oscillation of the conduction band electrons of the NPs is induced by light irradiation, and the oscillation generates a local electric field on the NP surface [9,10]. The intensity of the induced electric field near the surface of a plasmonic NP is enhanced at interstices between neighboring NPs at so-called "hotspots," as compared to the near-fields of individual NPs [11,12].

To efficiently utilize this collective property of plasmonic NPs (e.g. enhancement of Raman intensities [13–15], light trapping behaviors in solar cells and photocatalysts [16,17], and optical magnetism in metamaterials [18,19]), assembly of the NPs in a confined space is required [20]. Top-down approaches [21–26] such as lithography and bottom-up approaches [26–28] such as template-assisted self-assembly of the NPs have been employed to assemble the NPs on a substrate. Assembly of NPs can be dynamically controlled in a liquid phase using external stimuli. Solution pH and temperature, light, electric fields, and magnetic fields have been the focus of attention in recent years [20,29]. An external AC electric field is a powerful tool to assemble the NPs because it has many controllable parameters to modify the assembled states of NPs such as field strength, frequency, and application time.

Our previous report [30] demonstrated that Au NP clusters with different sizes were formed in a liquid phase by application of an electric field. The plasmonic properties of the Au NP clusters were strongly correlated with the number of Au NPs in the clusters. A high frequency field induced the formation of small clusters which successfully enhanced Raman intensities, showing that formation of clusters with a limited number of the Au NPs is useful to improve their properties. However, strong van der Waals forces between the clusters readily form bulk-like aggregates, inducing a decrease of the specific plasmonic properties of nano-sized particles.

The NPs dispersed in a medium, meanwhile, are preferred for sensing applications since all the NP surfaces are exposed and can efficiently combine with the targeting molecules. Additionally, Haes and co-workers [31,32] demonstrated that solution-phase measurement for SERS exhibited high reproducibility, resulting in a quantitative detection. In the present work, therefore, Au NP clusters with a limited number are intentionally encapsulated into a hollow silica sphere to keep them from aggregating in the liquid. Silica is chosen as encapsulating material for its high colloidal stability and high processability. Encapsulating the NPs into hollow spheres is also a useful way to keep the NP surfaces free from direct contact with other materials [33–36]. Assembled and dispersed states of the hollow silica spheres incorporating the Au NP clusters in water are controlled by switching an external AC electric field ON/OFF. Plasmonic properties of the dispersion are compared between conditions in the presence and the absence of the electric field.

2. Materials and methods

2.1. Materials

Hydrogen tetrachloroaurate(III) tetrahydrate ($HAuCl_4 \cdot 4H_2O$, 99.9%), trisodium citrate dihydrate (Na-cit·$2H_2O$, 99%), 4-mercaptobenzoic acid (PMBA, >95.0%), tetraethyl orthosilicate (TEOS, 95%), aqueous ammonia solution (NH_3, 25 wt%), and ethanol (99.5%) were purchased from FUJIFILM Wako Pure Chemical Corporation (Osaka, Japan). Polyethylenimine (PEI, M_W : ~25,000 g/mol) was purchased from Sigma-Aldrich (Tokyo, Japan). Water was deionized in advance (>18.2 MΩ cm).

2.2. Overview of the particle synthesis

Fig. 1 illustrates the synthesis scheme of hollow silica spheres incorporating multiple Au NPs (m-Au@hSiO_2). Au NPs modified with PMBA, probe molecules for Raman measurement, were coated with silica (m-Au@SiO_2) (i). The surfaces of m-Au@SiO_2 were then modified with the cationic polymer PEI (ii), and finally etched with water at 50 °C (iii). The detailed procedures of each synthesis are described in the following.

2.3. Synthesis of silica spheres incorporating Au NPs

Citrate-stabilized Au NPs with a size of 32 nm were synthesized according to previous reports [37,38]. To enable the investigation of the relation between assembled states of the hollow spheres incorporating Au NP clusters and Raman intensities, the citrate-stabilized Au NPs were first modified with PMBA as a Raman tag [39]. The PMBA-modified Au NPs were employed for the direct silica coating previously reported by our group [40]. The details of the synthesis procedure for the silica coating are given in Fig. S1. In order to control the number of Au NPs incorporated into a silica sphere, the concentration of Au NPs was tuned by the initial concentration of Au^{3+} in the synthesis reaction for Au NPs. Silica particles incorporating a single Au NP and those incorporating multiple Au NPs, synthesized at Au NP concentrations of 0.31 mM and 0.42 mM, respectively, are referred to as Au@SiO_2 and m-Au@SiO_2, respectively. The concentrations of elements measured with ICP-MS are summarized in Table S1 in the Supporting Information.

2.4. Synthesis of hollow silica spheres incorporating Au NPs

The hollow silica spheres incorporating Au NPs were synthesized by a "surface-protected etching process [41–44]," which is a procedure for the synthesis of hollow silica spheres using polymer with high molecular weight, PEI [43]. An ethanol solution of PEI was mixed with the ethanol solution of (m-)Au@SiO_2 in a vial by sonication for 15 min. The vial was transferred to a water bath, and then stirred at 35 °C for 30 min. The concentrations of PEI and (m-)Au@SiO_2 particles were 10 g/L (approximately 0.4 mM) and 5.3×10^{-4} vol%, respectively. After centrifugation the (m-)Au@SiO_2 particles modified with PEI were redispersed in water. The aqueous suspension was stirred at 50 °C for 15 h, after which the particles were washed twice more with water. Hollow silica spheres incorporating a single Au NP and those incorporating multiple Au NPs are referred to as Au@hSiO_2 and m-Au@hSiO_2, respectively.

2.5. Measurement of Raman spectra under application of an external AC electric field

Fig. 2 shows the schematic procedure for Raman measurement of (m-)Au@hSiO_2 aqueous suspensions to which an external AC

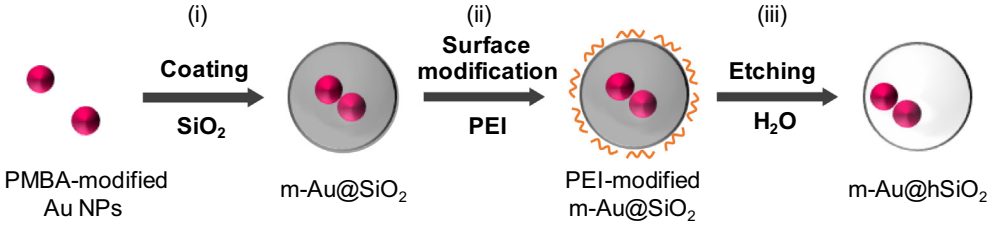

Fig. 1. Synthesis scheme of a hollow silica particle incorporating multiple Au NPs (m-Au@hSiO$_2$).

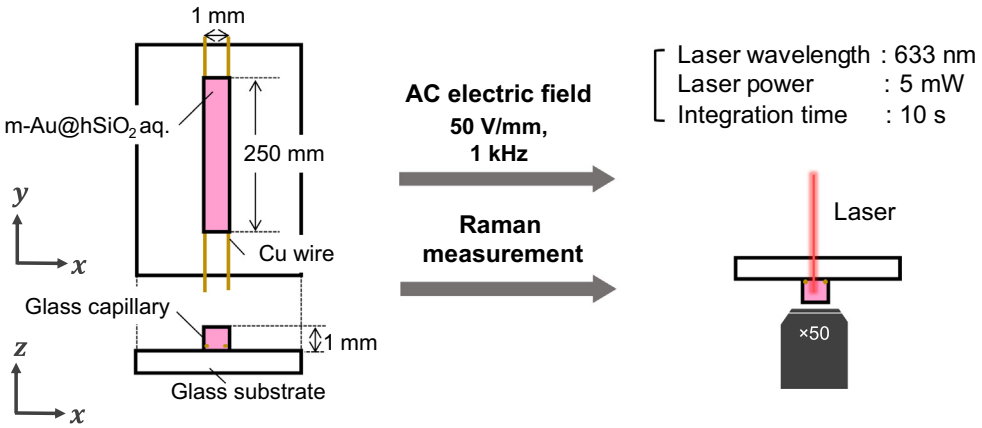

Fig. 2. Schematic procedure of Raman measurement under application of an AC electric field.

field was applied during the measurement. Each suspension, with a concentration was 0.15 vol%, was sealed in a glass capillary (Vitro-Com, Miniature Hollow Glass (1 mm × 1 mm)) with a UV glue. An external AC field was applied to the Au NP suspension with a function generator (HP 33120A) and amplifier (Krohn-Hite, 7602 M). The electric field strength (peak to peak) was measured via a digital oscilloscope (Tektronix, TDS3052). The Raman spectra of PMBA were measured via a confocal Raman microscope (Renishaw, inVia) under the application of an AC field at 1 kHz and the field strength for 50 V/mm. Measurement with a 50X objective lens was performed using a 633 nm laser with a 5 mW incident power and an integration time of 10 s.

2.6. Observation of Au NPs incorporated into a hollow silica sphere

The mobility of Au NPs contained within a hollow silica sphere filled with water was observed with liquid cell transmission electron microscopy (LCTEM) the concept of which was proposed by Williamson *et al.* in 2003 [45]. The details of LCTEM are presented in the Supporting information.

2.7. Calculation of the intensity of electric fields induced between Au NPs in a hollow sphere

The light-induced electric fields induced between Au NPs in a hollow silica sphere were calculated with a finite element method (FEM) using COMSOL Multiphysics® (version 5.3). In the calculation, the sizes of the Au NP, the hollow silica sphere, and thickness of the hollow silica shell were assumed as 30 nm, 186 nm, and 5 nm, respectively. The distance between Au NPs was 1 nm, which was assumed because of the approximate size of the PMBA molecules [46]. The details of the calculation are shown in the Supporting information.

2.8. Characterization

Synthesized particles were observed with a FE-TEM (Hitachi, HD-2700). UV–Vis spectra of the particle suspensions were measured with a UV–Vis spectrometer (Hitachi, U-3900). Under the application of an electric field, UV–Vis spectra of the suspensions were measured with another UV–Vis spectrometer (Agilent Technologies, Agilent Cary 8454). The volume-averaged diameter (d_V) and the coefficient of variation of particle size distribution (C_V) were calculated using equation (1) and (2), respectively.

$$d_V = \left(\sum n_i d_i^3 / \sum n_i\right)^{1/3} \tag{1}$$

$$C_V = \frac{\left[\sum \{d_i - (\sum n_i d_i / \sum n_i)\}^2\right]^{1/2}}{\sum n_i d_i / \sum n_i} \times 100 \tag{2}$$

where n_i is the number of particles with diameter d_i which were determined by measuring more than 200 particles in TEM images.

3. Results and discussion

3.1. Silica spheres incorporating Au NPs

Fig. 3(a) and (c) show TEM images of silica spheres incorporating Au NPs acquired at different Au NP concentrations of 0.31 mM and 0.42 mM, respectively. The distributions of the number of Au NPs incorporated into a silica sphere were estimated by counting more than 200 particles in the TEM images (Fig. 3(b) and (d)). Almost 90% of the silica spheres contained a single Au NP in the case of 0.31 mM (Au@SiO$_2$), whereas approximately 40% of the silica spheres encapsulated multiple Au NPs with different numbers ranging 2–10 in the case of 0.42 mM (m-Au@SiO$_2$). It was difficult that the number of Au NPs incorporated into the silica spheres was exactly controlled due to random slow coagulation of the NPs in

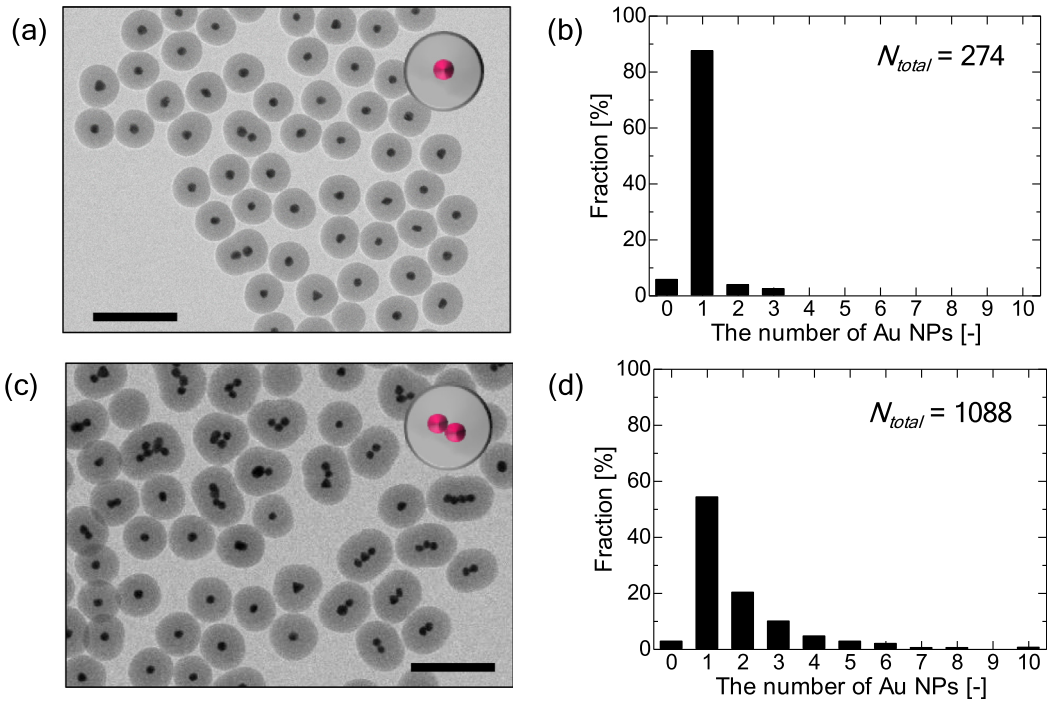

Fig. 3. TEM images of (m-)Au@SiO_2 and the number distributions of Au NPs in a silica particle prepared at different Au NP concentrations of 0.31 mM (a, b) and 0.42 mM (c, d). All scale bars are 300 nm.

the synthesis. The TEM images of silica spheres incorporating Au NPs synthesized with other Au NP concentrations (0.21–0.38 mM) are shown in Fig. S5. Interestingly, most Au NPs in the silica sphere formed chain-like structures (see again Fig. 3(c)). This is presumably due to the electrostatic repulsion between the NP chains and surrounding NPs. According to previous reports [47–49], the electrostatic repulsion force of the sides of the NP chains can be bigger than the ends of the chain, resulting in the formation of the chain-like structures rather than clusters.

The UV–Vis spectra of individual Au NPs, Au@SiO_2, and m-Au@SiO_2 are presented in Fig. 4. The extinction peaks of the aqueous suspensions of silica coated Au NPs (solid lines) were red-shifted compared to dispersed Au NPs (dashed line). The red-shift can be explained by considering the difference in refractive index between the silica shells (n = 1.45) and water (n = 1.33) surrounding the Au NPs [39,50–52]. Both Au@SiO_2 and m-Au@SiO_2 exhibited almost the same extinction peak at approximately 542 nm, whereas the spectrum of m-Au@SiO_2 also showed a second peak at wavelengths longer than the first peak wavelength. This indicated that hotspots were created between the Au NPs in the hollow silica spheres in the case of m-Au@SiO_2.

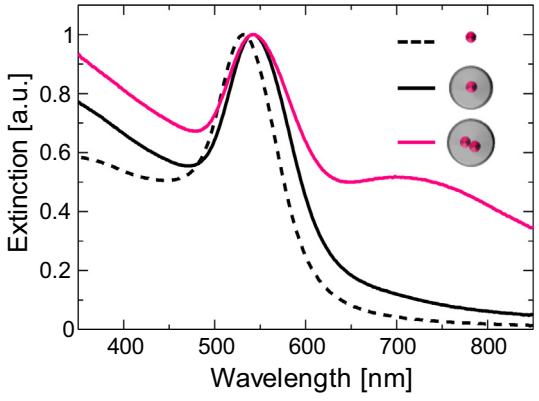

Fig. 4. UV–Vis spectra of aqueous suspensions of Au NPs (dashed black line), Au@SiO_2 (black line), and m-Au@SiO_2 (pink line). (For interpretation of the references to colour in this figure legend, the reader is referred to the web version of this article.)

3.2. Hollow silica spheres incorporating Au NPs

The TEM images of the hollow silica spheres obtained after the selective etching of Au@SiO_2 and m-Au@SiO_2 using PEI are shown in Fig. 5(a) and (b). The average diameter (d_V) of Au@hSiO_2 and m-Au@hSiO_2 particles were 151 nm and 186 nm, respectively. The silica shell thickness of the hollow spheres was approximately 5 nm, which was estimated from the TEM images. Because PEI can protect the outer surface of the silica shell, the inner part of silica spheres can be selectively removed in water. The solution pH of the aqueous suspension of PEI-modified Au@SiO_2 measured before the etching process was approximately 10, suggesting that inner silica shells can be dissolved in the basic solution [53].

Fig. 5(c) shows UV–Vis spectra of aqueous suspensions of Au@hSiO_2 and m-Au@hSiO_2. The extinction peaks were both at approximately 530 nm, which was almost the same as for dispersed Au NPs in water, meaning that the inner part of silica spheres was successfully removed. The Au NPs are probably close to each other inside the hollow sphere even after the etching process because the spectra of m-Au@hSiO_2 broadened to longer wavelengths similar to those of m-Au@SiO_2 shown in Fig. 4.

Fig. 5(d) presents Raman spectra of PMBA measured in aqueous suspensions of Au@hSiO_2 and m-Au@hSiO_2. Even though PMBA was chemically anchored to Au NP surfaces in the synthesis process, no specific peaks of PMBA were observed from Au@hSiO_2 whereas several peaks were observed in the presence of m-Au@hSiO_2 (see Table S2 for the details). This suggests that incorporation of multiple Au NPs into hollow spheres can enhance the SERS effect due to the hotspots created between multiple Au NPs, even if the total concentration of m-Au@hSiO_2 in solution was low (0.15 vol%).

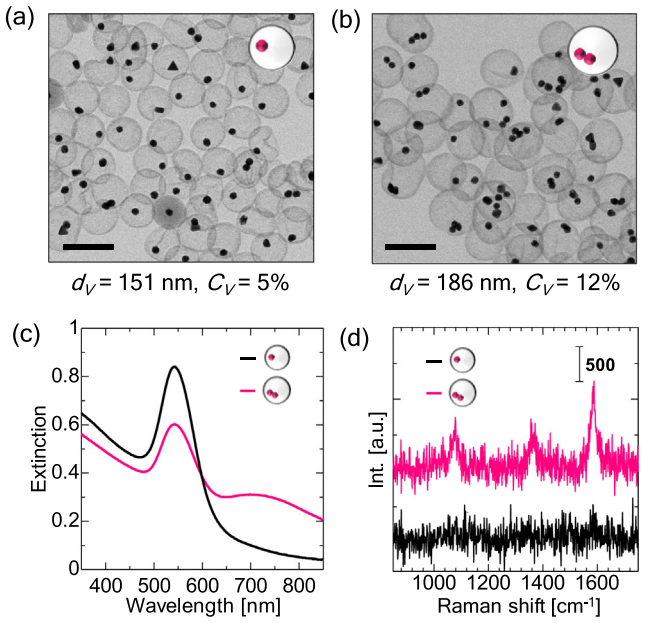

Fig. 5. TEM images of Au@hSiO$_2$ (a) and m-Au@hSiO$_2$ (b). All scale bars are 300 nm. UV–Vis spectra of (m-)Au@hSiO$_2$ (c) and Raman spectra of PMBA in the presence of (m-)Au@hSiO$_2$ (d).

3.3. Observation of the mobility of Au NPs incorporated into a hollow silica sphere in water

Fig. 6 shows stills of Movie S1 observed with LCTEM for multiple Au NPs inside a hollow silica sphere in water. As shown in the movie and in the stills, two connected Au NPs moved as one Au NP cluster within the confines of the hollow sphere, instead of as two separate Au NPs. Four Au NPs in a hollow sphere in the same Movie S1 also exhibited the movement as a cluster, which is probably held together by strong van der Waals interactions. This result is in agreement with the UV–Vis spectra in Fig. 5(c), which featured a peak at longer wavelengths (600–800 nm) due to plasmonic coupling between the Au NPs is present within the hollow compartment.

3.4. Finite element calculations on the light-induced electric field enhancement between the Au NPs incorporated into a hollow sphere

To provide computational evidence for the creation of hotspots between the Au NPs in the clusters, the electric fields between the Au NPs in the hollow sphere induced by light were calculated using COMSOL Multiphysics®. Fig. 7(a) to (c) show the induced electric fields surrounding a single Au NP, Au NP dimer, and tetramer, respectively. The induced electric fields between clusters consisting of Au NPs with different numbers and assembled structures are shown in Fig. S6 in the Supporting information. The same irradiating wavelength as the laser for Raman spectroscopy, 633 nm, was used for this calculation. The maximum intensity of the electric field at the interstice of the Au dimer was more than 300 V/m (see Fig. S4), much higher than that at a single Au NP (approximately 4.5 V/m), which suggested that hotspots were created between Au NPs in the cluster. Because the LSPR wavelength of the Au NP tetramer is longer than that of the dimer [54], the intensity of the induced electric field between NPs in the tetramer was approximately 200 V/m, which was lower than that of the Au NP dimer. Almost 20% of the hollow spheres were encapsulating Au NP dimers in the synthesis condition for m-Au@hSiO$_2$ (see again Fig. 3(d)), and thereby the SERS effect can be efficiently enhanced for 633-nm light.

3.5. Assembling Au NP clusters encapsulated into hollow spheres by an external electric field

Assembling the Au NPs incorporated into hollow spheres in an even more confined space allows enhancing and tuning of their collective properties. Here, an external electric field was applied to the aqueous suspension of (m-)Au@hSiO$_2$ to locally gather the particles, and Raman intensities acquired under the electric field were investigated. Fig. 8(a) and (b) show Raman spectra of PMBA acquired under an electric field at 50 V/mm (1 kHz) in the presence of Au@hSiO$_2$ and m-Au@hSiO$_2$, respectively. Weak PMBA peaks were observed in the case of Au@hSiO$_2$ after 10 min of the field application, whereas the intensities of the specific peaks clearly increased more with application time in the case of m-Au@hSiO$_2$ as shown in Fig. 8(b). It shows that the electric field-assisted assembling of the Au NP clusters was effective for the enhancement of Raman intensities because of the hotspots created between the NPs.

The enhancement of Raman intensities is mainly caused by the dielectrophoretic force, which can capture dispersed particles near electrodes in a liquid phase [55–57]. Fig. S7 shows optical microscopy images of the aqueous suspension of (m-)Au@hSiO$_2$ in the vicinity of the electrode and the central part of the glass capillary, taken 10 min after application of the electric field at 50 V/mm. Although the hollow spheres were too small to be clearly distinguished with the optical microscope, the concentrated assemblies of (m-)Au@hSiO$_2$ were clearly observed near the electrode after switching on the electric field. Fig. S8 shows UV–Vis spectra of the aqueous suspensions of (m-)Au@hSiO$_2$ acquired with electric field during 10 min. The extinction peaks around 530 nm gradually weakened during this period of time due to dielectrophoresis of the (m-)Au@hSiO$_2$ toward the electrodes. However, no peak shifts were observed in the spectra, suggesting that no hotspots were created between the Au NP clusters incorporated into different hollow spheres. The results revealed that distinct Raman peaks can be acquired by increasing the number density of the Au NP clusters in an area onto which the laser of Raman spectroscope was focused.

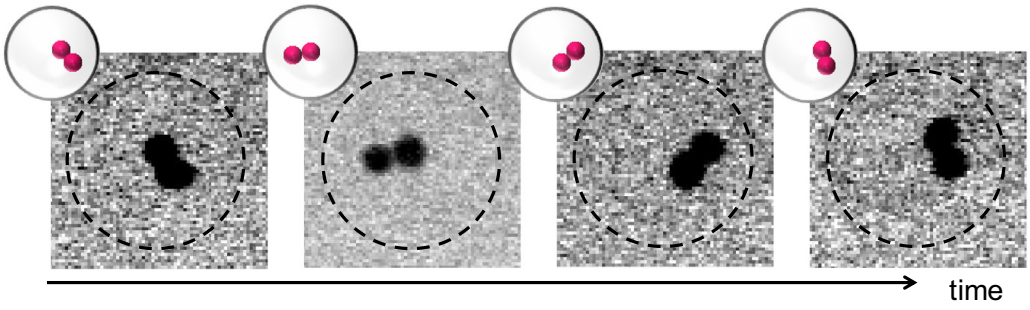

Fig. 6. Snapshots of a movie capturing the movement of two Au NPs in a silica sphere observed with LCTEM. Dashed lines show the hollow silica sphere.

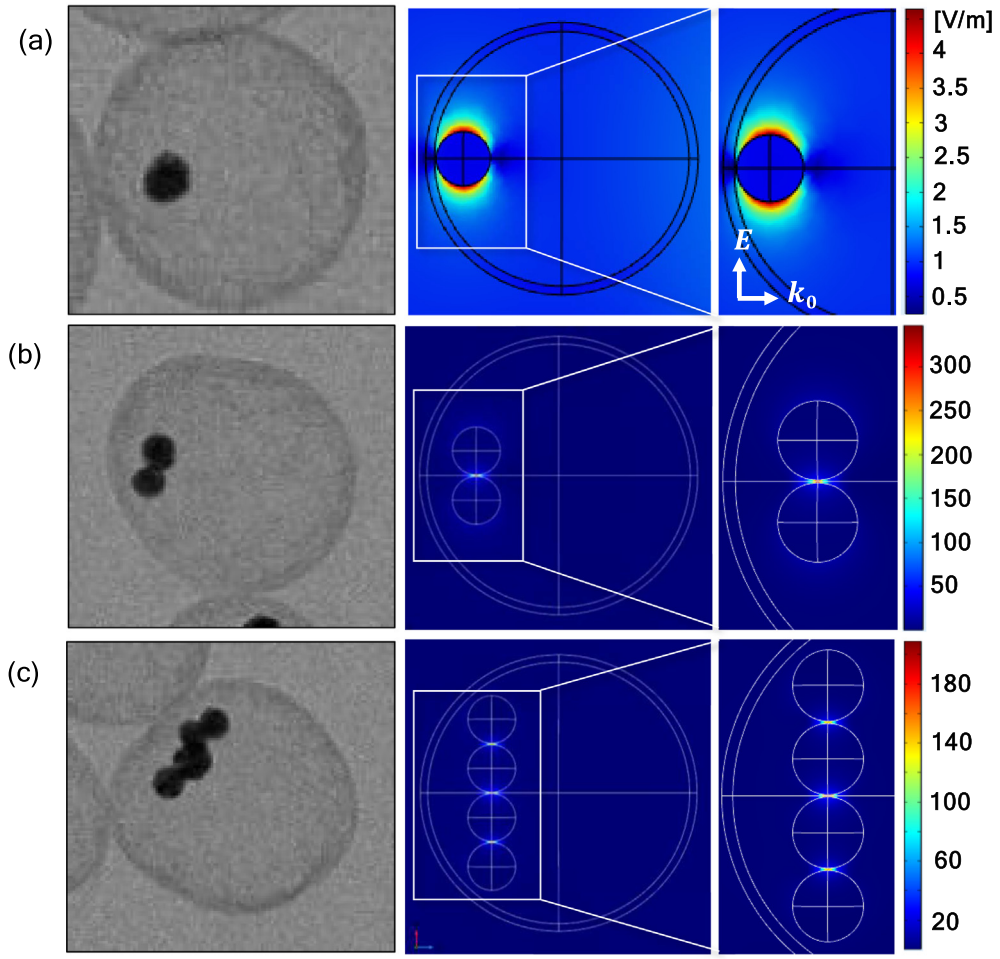

Fig. 7. EM images and electric field mappings induced by irradiation of light at 633 nm. Hollow silica spheres incorporating Au NP monomer (a), dimer (b), and tetramer (c).

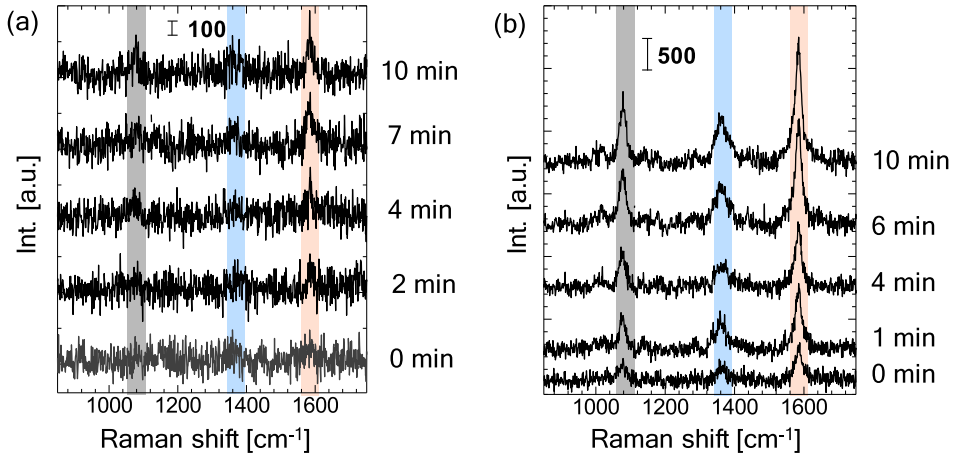

Fig. 8. Raman spectra of PMBA observed under application of an electric field at 50 V/mm at 1 kHz for different application times ranging from 0 to 10 min in the presence of Au@hSiO$_2$ (a) and m-Au@hSiO$_2$ (b).

In the present work, the probe molecules, PMBA, were chemically anchored on the Au NP surface in advance to investigate the relationship between the assembled state of m-Au@hSiO$_2$ and the effect of the Raman enhancement. The proposed method to efficiently utilize the collective properties of the NPs using external electric fields can be employed for practical applications such as biosensors by encapsulating the NP clusters within hollow silica shells having large pores permeable by the probe molecules.

3.6. Reversible increasing concentration of hollow silica spheres encapsulating Au NP clusters by dielectrophoresis

The external electric field was switched ON/OFF several times to examine the reversibility of the process. As shown in Fig. 9(a), distinct peaks of PMBA were acquired after field application for 10 min, and the peak enhancement was repeatedly observed by switching the electric field ON/OFF. This supports that the hollow

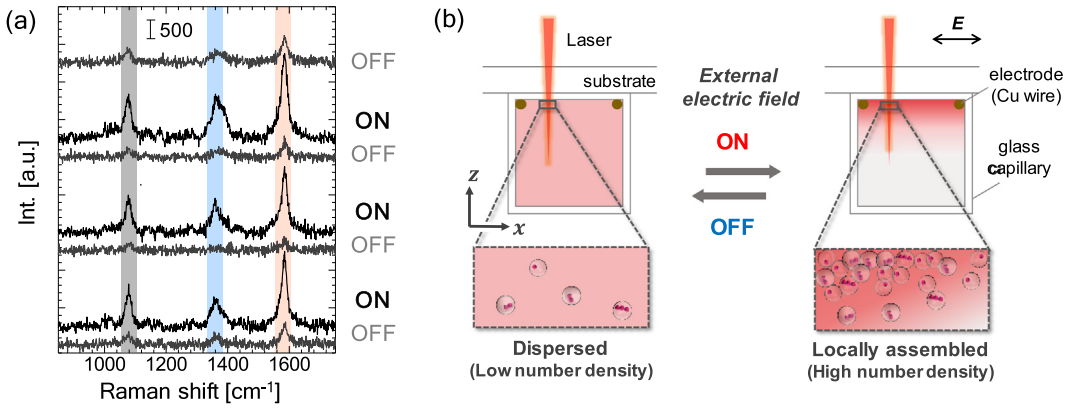

Fig. 9. Raman spectra of PMBA observed with and without application of an electric field of 50 V/m at 1 kHz (a). The spectra at ON states were measured after 10 min of field application. The spectra at OFF states were measured 30 min after turning off the electric field. Schematic diagrams of the transition between the dispersed state and locally assembled state of m-Au@hSiO$_2$ in water (b).

silica spheres incorporating Au NPs disperse again even once the hollow spheres were attracted close to each other by the external electric fields (see the schematic diagram shown in Fig. 9(b)). The reversible transition between the assembled states and the dispersed states of the hollow particles can be quickly induced by switching the electric field ON/OFF, which is an advantage in the present work over other methods using sedimentation or centrifugation for particle assembly.

The reversibility of the transition between the assembled and dispersed states of the Au NP clusters in hollow silica compartments showed that the hollow spheres, having a high colloidal stability, can act as a physical barrier for avoiding further aggregation of the NP clusters. Our previous report [30], which demonstrated the difficulty of maintaining the dispersed state of the NP clusters in suspension, supports that the compartmentalization of unstable NP clusters within hollow shells can be a promising way to keep them stable in the liquid. The stabilized clusters with plasmonic hotspots that can be reversibly concentrated by electric field gradients can lead to the development of reusable nanomaterials such as sensing devices and batteries.

4. Conclusions

Hollow silica spheres incorporating gold nanoparticles were synthesized by a surface-protected etching process using polyethylenimine. Approximately 40% of the hollow spheres encapsulated multiple gold nanoparticles with numbers varying from 2 to 10. Observation with liquid cell transmission electron microscopy proved that multiple gold nanoparticles moved as a cluster instead of as dispersed nanoparticles inside the hollow sphere. Synthesis of hollow spheres incorporating a single nanoparticle [58–61] or dispersed multiple nanoparticles [62] have been previously reported by other research groups. The present work succeeded in encapsulation of mobile nanoparticle clusters into hollow silica spheres for the first time. The nanoparticle-cluster-containing hollow spheres were asembled in the vicinity of electrodes by application of an external electric field, resulting in enhancement of Raman intensities of probe molecules. The assembled hollow spheres were redispersed by turning off the electric field. The Raman intensity observed after the turning off the electric field was similar to that observed before the application of the electric field. It revealed that the Raman intensities depended on the number density of the nanoparticle clusters in a specific space. The assembled and dispersed states of the hollow spheres were reversibly controlled by switching the electric field on and off, indicating that the hollow spheres provided nano-sized compartments to keep the nanoparticles clusters dispersed in a liquid. Encapsulating the nanoparticle clusters into hollow silica spheres is a promising way for the clusters to physically avoid being aggregated during concentrating the clusters by using external stimuli such as electric fields and magnetic fields.

In order to acquire their uniform plasmonic properties from the nanoparticle clusters encapsulated in hollow spheres, the number of nanoparticles in a cluster needs to be accurately controlled. Plasmon resonance wavelengths of the clusters depend on the number of the nanoparticles in a cluster. Because light with appropriate wavelengths for the clusters can be employed, the hollow spheres with incorporating the clustered nanoparticles highly controlled are promising materials for various applications (e.g. photothermal therapy, bio sensing, optics, and batteries).

CRediT authorship contribution statement

Kanako Watanabe: Conceptualization, Validation, Investigation, Writing - original draft, Funding acquisition. **Tom A.J. Welling:** Validation, Investigation, Writing - review & editing. **Sina Sadighikia:** Validation, Investigation, Writing - review & editing. **Haruyuki Ishii:** Resources, Supervision, Writing - review & editing. **Arnout Imhof:** Writing - review & editing, Supervision. **Marijn A. Huis:** Resources, Writing - review & editing, Supervision, Funding acquisition. **Alfons Blaaderen:** Resources, Writing - review & editing, Supervision, Funding acquisition. **Daisuke Nagao:** Resources, Writing - review & editing, Supervision, Project administration, Funding acquisition.

Declaration of Competing Interest

The authors declare that they have no known competing financial interests or personal relationships that could have appeared to influence the work reported in this paper.

Acknowledgements

The authors thank technical support staff in the department of Engineering for the measurements, Tohoku University for STEM images. This research was mainly supported by the Ministry of Education, Culture, Sports, Science and Technology (JSPS KAKENHI Grant Numbers 16J03375, 15KK0222, 17H02744, 17K19020). MvH acknowledges the European Research Council for an ERC-CoG grant (NANO-INSITU, No. 683076).

Author contribution

KW designed the study, synthesized particles, did most of the measurement, and wrote the initial draft of the manuscript. TW and SS contributed to the observation and analysis using LCTEM. TW also assisted in the preparation of the manuscript. HI, AI, MvH, AvB, and DN advised for all experiments and analysis. All other authors have contributed to data collection, and critically reviewed the manuscript. All authors approved the final version of the manuscript.

Appendix A. Supplementary material

Movie of the LCTEM observation of Au NP clusters incorporated into hollow silica spheres in water (Movie 1). Mass of each element of (m-)Au@SiO_2 measured by ICP-MS (Table S1), and Raman peaks of PMBA acquired in the aqueous suspension of m-Au@hSiO_2 (Table S2). The detailed synthesis procedure of (m-)Au@SiO_2 (Fig. S1), a schematic of the setup of the LCTEM (Fig. S2), the dimension of a Au NP dimer incorporated into a hollow silica sphere for FED calculations (Fig. S3), electric field mappings and calculated intensity of the fields between Au NPs induced by irradiation of light at 633 nm (Fig. S4), the TEM images of (m-)Au@SiO_2 synthesized by adjusting Au NP concentrations ranging from 0.21 to 0.38 mM (Fig. S5), and electric field mappings between Au NPs in various clusters induced by irradiation of light at 633 nm (Fig. S6). Optical microscope images of the aqueous suspensions of (m-)Au@SiO_2 and UV-Vis spectra measured after the application of the electric field for 10 min (Figs. S7, S8). The electric field mapping between the hollow silica spheres incorporating Au NP dimers (Fig. S9). Supplementary data to this article can be found online at https://doi.org/10.1016/j.jcis.2020.01.094.

References

[1] D. Astruc, F. Lu, J.R. Aranzaes, Nanoparticles as recyclable catalysts: the frontier between homogeneous and heterogeneous catalysis, Angew. Chemie – Int. Ed. 44 (2005) 7852–7872, https://doi.org/10.1002/anie.200500766.

[2] Y. Yamamoto, H. Hori, Direct observation of the ferromagnetic spin polarization in gold nanoparticles: a review, Rev. Adv. Mater. Sci. 12 (2006) 23–32, https://doi.org/10.1103/PhysRevLett. 93.116801.

[3] K.L. Kelly, E. Coronado, L.L. Zhao, G.C. Schatz, The optical properties of metal nanoparticles: the influence of size, shape, and dielectric environment, J. Phys. Chem. B 107 (2003) 668–677, https://doi.org/10.1021/jp026731y.

[4] V. Sharma, K. Park, M. Srinivasarao, Colloidal dispersion of gold nanorods: Historical background, optical properties, seed-mediated synthesis, shape separation and self-assembly, Mater. Sci. Eng. R Reports 65 (2009) 1–38, https://doi.org/10.1016/j.mser.2009.02.002.

[5] M. Fleischmann, P.J. Hendra, A.J. McQuillan, Raman spectra of pyridine adsorbed at a silver electrode, Chem. Phys. Lett. 26 (1974) 163–166, https://doi.org/10.1016/0009-2614(74)85388-1.

[6] D.L. Jeanmaire, R.P. Van Duyne, Surface raman spectroelectrochemistry: Part I. Heterocyclic, aromatic, and aliphatic amines adsorbed on the anodized silver electrode, J. Electroanal. Chem. 84 (1977) 1–20, https://doi.org/10.1016/S0022-0728(77)80224-6.

[7] K. Kneipp, H. Kneipp, V. Kartha, R. Manoharan, G. Deinum, I. Itzkan, R. Dasari, M. Feld, Detection and identification of a single DNA base molecule using surface-enhanced Raman scattering (SERS), Phys. Rev. E 57 (1998) 6281–6284, https://doi.org/10.1103/PhysRevE.57.R6281.

[8] S. Shanmukh, L. Jones, J. Driskell, Y.P. Zhao, R. Dluhy, R.a. Tripp, Rapid and sensitive detection of respiratory virus molecular signatures using a silver nanorod array SERS substrate, Nano Lett. 6 (2006) 2630–2636, https://doi.org/10.1021/Nl061666f.

[9] E. Hutter, J.H. Fendler, Exploitation of localized surface plasmon resonance, Adv. Mater. 16 (2004) 1685–1706, https://doi.org/10.1002/adma.200400271.

[10] K.M. Mayer, J.H. Hafner, Localized surface plasmon resonance sensors, Chem. Rev. 111 (2011) 3828–3857, https://doi.org/10.1021/cr100313v.

[11] E. Hao, G.C. Schatz, Electromagnetic fields around silver nanoparticles and dimers, J. Chem. Phys. 120 (2004) 357–366, https://doi.org/10.1063/1.1629280.

[12] P.Z. El-Khoury, E. Khon, Y. Gong, A.G. Joly, P. Abellan, J.E. Evans, N.D. Browning, D. Hu, M. Zamkov, W.P. Hess, Electric field enhancement in a self-assembled 2D array of silver nanospheres, J. Chem. Phys. 141 (2014) 214308, https://doi.org/10.1063/1.4902905.

[13] W. Rechberger, A. Hohenau, A. Leitner, J.R. Krenn, B. Lamprecht, F.R. Aussenegg, Optical properties of two interacting gold nanoparticles, Opt. Commun. 220 (2003) 137–141, https://doi.org/10.1016/S0030-4018(03)01357-9.

[14] S.-Y. Ding, E.-M. You, Z.-Q. Tian, M. Moskovits, Electromagnetic theories of surface-enhanced Raman spectroscopy, Chem. Soc. Rev. 46 (2017) 4042–4076, https://doi.org/10.1039/C7CS00238F.

[15] W. Li, P.H.C. Camargo, X. Lu, Y. Xia, Dimers of silver nanospheres: Facile synthesis and their use as hot spots for surface-enhanced raman scattering, Nano Lett. 9 (2009) 485–490, https://doi.org/10.1021/nl803621x.

[16] S.V. Boriskina, H. Ghasemi, G. Chen, Plasmonic materials for energy: from physics to applications, Mater. Today 16 (2013) 375–386, https://doi.org/10.1016/j.mattod.2013.09.003.

[17] H. Tan, R. Santbergen, A.H.M. Smets, M. Zeman, Plasmonic light trapping in thin-film silicon solar cells with improved self-assembled silver nanoparticles, Nano Lett. 12 (2012) 4070–4076, https://doi.org/10.1021/nl301521z.

[18] Z. Qian, S.P. Hastings, C. Li, B. Edward, C.K. McGinn, N. Engheta, Z. Fakhraai, S.J. Park, Raspberry-like metamolecules exhibiting strong magnetic resonances, ACS Nano 9 (2015) 1263–1270, https://doi.org/10.1021/nn5050678.

[19] S.N. Sheikholeslami, H. Alaeian, A.L. Koh, J.A. Dionne, A metafluid exhibiting strong optical magnetism, Nano Lett. 13 (2013) 4137–4141, https://doi.org/10.1021/nl401642z.

[20] Z. Qian, D.S. Ginger, Reversibly reconfigurable colloidal plasmonic nanomaterials, J. Am. Chem. Soc. 139 (2017) 5266–5276, https://doi.org/10.1021/jacs.7b00711.

[21] M. Jahn, S. Patze, I.J. Hidi, R. Knipper, A.I. Radu, A. Mühlig, S. Yüksel, V. Peksa, K. Weber, T. Mayerhöfer, D. Cialla-May, J. Popp, Plasmonic nanostructures for surface enhanced spectroscopic methods, Analyst 141 (2016) 756–793, https://doi.org/10.1039/C5AN02057C.

[22] A. Shiohara, Y. Wang, L.M. Liz-Marzán, Recent approaches toward creation of hot spots for SERS detection, J. Photochem. Photobiol. C Photochem. Rev. 21 (2014) 2–25, https://doi.org/10.1016/j.jphotochemrev.2014.09.001.

[23] A. Gopinath, S.V. Boriskina, N.N. Feng, B.M. Reinhard, L. Dal Negro, Photonic-plasmonic scattering resonances in deterministic aperiodic structures, Nano Lett. 8 (2008) 2423–2431, https://doi.org/10.1021/nl8013692.

[24] R. Winkler, F.P. Schmidt, U. Haselmann, J.D. Fowlkes, B.B. Lewis, G. Kothleitner, P.D. Rack, H. Plank, Direct-Write 3D Nanoprinting of Plasmonic Structures, ACS Appl. Mater. Interfaces 9 (2017) 8233–8240, https://doi.org/10.1021/acsami.6b13062.

[25] K. Dietrich, D. Lehr, C. Helgert, A. Tünnermann, E.B. Kley, Circular dichroism from chiral nanomaterial fabricated by on-edge lithography, Adv. Mater. 24 (2012) 321–325, https://doi.org/10.1002/adma.201203424.

[26] J.P. Camden, J.A. Dieringer, J. Zhao, R.P. Van Duyne, Controlled plasmonic nanostructures for surface-enhanced spectroscopy and sensing, Acc. Chem. Res. 41 (2008) 1653–1661, https://doi.org/10.1021/ar800041s.

[27] M. Mayer, M. Tebbe, C. Kuttner, M.J. Schnepf, T.A.F. König, A. Fery, Template-assisted colloidal self-assembly of macroscopic magnetic metasurfaces, Faraday Discuss. 191 (2016) 159–176, https://doi.org/10.1039/C6FD00013D.

[28] E.M. Hicks, O. Lyandres, W. Paige Hall, S. Zou, M.R. Glucksberg, R.P. Van Duyne, Plasmonic properties of anchored nanoparticles fabricated by reactive ion etching and nanosphere lithography, J. Phys. Chem. C 111 (2007) 4116–4124, https://doi.org/10.1021/jp064094w.

[29] K. Watanabe, K. Kuroda, D. Nagao, External-stimuli-assisted control over assemblies of plasmonic metals, Materials (Basel) 11 (2018) 794, https://doi.org/10.3390/ma11050794.

[30] K. Watanabe, E. Tanaka, H. Ishii, D. Nagao, The plasmonic properties of gold nanoparticle clusters formed: Via applying an AC electric field, Soft Matter 14 (2018) 3372–3377, https://doi.org/10.1039/c8sm00097b.

[31] M.C.S. Pierre, A.J. Haes, Purification implications on SERS activity of silica coated gold nanospheres, Anal. Chem. 84 (2012) 7906–7911, https://doi.org/10.1021/ac3016517.

[32] M. Roca, A.J. Haes, M. Roca, A.J. Haes, Silica # Void # Gold nanoparticles : temporally stable surface-enhanced raman scattering substrates silica - void - gold nanoparticles : temporally stable surface-enhanced raman scattering substrates, J. Am. Chem. Soc. 52242 (2008) 14273–14279, https://doi.org/10.1021/ja8059039.

[33] A. Okada, D. Nagao, T. Ueno, H. Ishii, M. Konno, Colloidal polarization of yolk/shell particles by recon fi guration of inner cores responsive to an external magnetic field, Langmuir 29 (2013) 9004–9009.

[34] A. Okada, D. Nagao, H. Ishii, M. Konno, Direct observation of micron-sized silica rattles to demonstrate movability of inner spheres in the silica compartment suspended in aqueous media, Soft Matter 8 (2012) 3442, https://doi.org/10.1039/c2sm06946f.

[35] K. Watanabe, H. Ishii, M. Konno, A. Imhof, A. van Blaaderen, D. Nagao, Yolk/shell colloidal crystals incorporating movable cores with their motion controlled by an external electric field, Langmuir 33 (2017) 296–302, https://doi.org/10.1021/acs.langmuir.6b03116.

[36] K. Watanabe, D. Nagao, H. Ishii, M. Konno, Rattle-type colloidal crystals composed of spherical hollow particles containing an anisotropic, movable core, Langmuir 31 (2015) 5306–5310, https://doi.org/10.1021/acs.langmuir.5b01148.

[37] B.V. Enustun, J. Turkevich, Coagulation of colloidal gold, J. Am. Chem. Soc. 85 (1963) 3317.

[38] N.G. Bastús, J. Comenge, V. Puntes, Kinetically controlled seeded growth synthesis of citrate-stabilized gold nanoparticles of up to 200 nm: Size focusing versus ostwald ripening, Langmuir 27 (2011) 11098–11105, https://doi.org/10.1021/la201938u.

[39] C. Wei, M.M. Xu, C.W. Fang, Q. Jin, Y.X. Yuan, J.L. Yao, Improving the sensitivity of immunoassay based on MBA-embedded Au@SiO2nanoparticles and surface enhanced Raman spectroscopy, Spectrochim. Acta – Part A Mol. Biomol. Spectrosc. 175 (2017) 262–268, https://doi.org/10.1016/j.saa.2016.12.036.
[40] E. Mine, A. Yamada, Y. Kobayashi, M. Konno, L.M. Liz-Marzán, Direct coating of gold nanoparticles with silica by a seeded polymerization technique, J. Colloid Interface Sci. 264 (2003) 385–390, https://doi.org/10.1016/S0021-9797(03)00422-3.
[41] Q. Zhang, J. Ge, J. Goebl, Y. Hu, Z. Lu, Y. Yin, Rattle-type silica colloidal particles prepared by a surface-protected etching process, Nano Res. 2 (2009) 583–591, https://doi.org/10.1007/s12274-009-9060-5.
[42] Y. Hu, Q. Zhang, J. Goebl, T. Zhang, Y. Yin, Control over the permeation of silica nanoshells by surface-protected etching with water, PCCP 12 (2010) 11836–11842, https://doi.org/10.1039/c0cp00031k.
[43] L. Zhang, T. Wang, L. Yang, C. Liu, C. Wang, H. Liu, Y.A. Wang, Z. Su, General route to multifunctional uniform yolk/mesoporous silica shell nanocapsules: a platform for simultaneous cancer-targeted imaging and magnetically guided drug delivery, Chem. – A Eur. J. 18 (2012) 12512–12521, https://doi.org/10.1002/chem.201200030.
[44] M.S. Islam, W.S. Choi, H.J. Lee, Controlled etching of internal and external structures of SiO2 nanoparticles using hydrogen bond of polyelectrolytes, ACS Appl. Mater. Interfaces 6 (2014) 9563–9571, https://doi.org/10.1021/am501941c.
[45] M.J. Williamson, R.M. Tromp, P.M. Vereecken, R. Hull, F.M. Ross, Dynamic microscopy of nanoscale cluster growth at the solid–liquid interface, Nat. Mater. 2 (2003) 532–536, https://doi.org/10.1038/nmat944.
[46] Z. Gao, N.D. Burrows, N.A. Valley, G.C. Schatz, C.J. Murphy, C.L. Haynes, In solution SERS sensing using mesoporous silica-coated gold nanorods, Analyst. 141 (2016) 5088–5095, https://doi.org/10.1039/c6an01159d.
[47] E.C. Cho, S.W. Choi, P.H.C. Camargo, Y. Xia, Thiol-induced assembly of au nanoparticles into chainlike structures and their fixing by encapsulation in silica shells or gelatin microspheres, Langmuir 26 (2010) 10005–10012, https://doi.org/10.1021/la100127w.
[48] H. Zhang, D. Wang, Controlling the growth of charged-nanoparticle chains through interparticle electrostatic repulsion, Angew. Chemie – Int. Ed. 47 (2008) 3984–3987, https://doi.org/10.1002/anie.200705537.
[49] M. Akbulut, A.R.G. Alig, Y. Min, N. Belman, M. Reynolds, Y. Golan, J. Israelachvili, Forces between surfaces across nanoparticle solutions: Role of size, shape, and concentration, Langmuir 23 (2007) 3961–3969, https://doi.org/10.1021/la062613g.
[50] C. Wang, Z. Ma, T. Wang, Z. Su, Synthesis, assembly, and biofunctionalization of silica-coated gold nanorods for colorimetric biosensing, Adv. Funct. Mater. 16 (2006) 1673–1678, https://doi.org/10.1002/adfm.200500898.
[51] W.E. Doering, S. Nie, spectroscopic tags using dye-embedded nanoparticles and surface-enhanced Raman scattering, Anal. Chem. 75 (2003) 6171–6176, https://doi.org/10.1021/ac034672u.
[52] Y. Qi, M. Chen, S. Liang, J. Zhao, W. Yang, Hydrophobation and self-assembly of core-shell Au@SiO2 nanoparticles, Colloids Surfaces A Physicochem. Eng. Asp. 302 (2007) 383–387.
[53] G.B. Alexander, W.M. Heston, R.K. Iler, The solubility of amorphous silica in water, J. Phys. Chem. 58 (1954) 453–455, https://doi.org/10.1021/j150516a002.
[54] C. Tira, D. Tira, T. Simon, S. Astilean, Finite-Difference Time-Domain (FDTD) design of gold nanoparticle chains with specific surface plasmon resonance, J. Mol. Struct. 1072 (2014) 137–143, https://doi.org/10.1016/j.molstruc.2014.04.086.
[55] R.C. Peter, J. Gascoyne, Vykoukal, Particle separation by dielectrophoresis, Electrophoresis 23 (2002) 1973–1983, https://doi.org/10.1002/1522-2683(200207)23:13<1973::AID-ELPS1973>3.0.CO;2-1.
[56] H.A. Pohl, The motion and precipitation of suspensoids in divergent electric fields, J. Appl. Phys. 22 (1951) 869–871, https://doi.org/10.1063/1.1700065.
[57] A. van Blaaderen, M. Dijkstra, R. van Roij, A. Imhof, M. Kamp, B.W. Kwaadgras, T. Vissers, B. Liu, Manipulating the self assembly of colloids in electric fields, Eur. Phys. J. Spec. Top. 222 (2013) 2895–2909, https://doi.org/10.1140/epjst/e2013-02065-0.
[58] K. Kamata, Y. Lu, Y. Xia, Synthesis and characterization of monodispersed core-shell spherical colloids with movable cores, J. Am. Chem. Soc. 125 (2003) 2384–2385, https://doi.org/10.1021/ja0292849.
[59] X. Li, L. Xing, K. Zheng, P. Wei, L. Du, M. Shen, X. Shi, Formation of gold nanostar-coated hollow mesoporous silica for tumor multimodality imaging and photothermal therapy, ACS Appl. Mater. Interfaces 9 (2017) 5817–5827, https://doi.org/10.1021/acsami.6b15185.
[60] M. Blanco-Formoso, A. Sousa-Castillo, X. Xiao, A. Marino-Lopez, M. Turino, N. Pazos-Perez, V. Giannini, M.A. Correa-Duarte, R.A. Alvarez-Puebla, Boosting the analytical properties of gold nanostars by single particle confinement into yolk porous silica shells, Nanoscale 21872–21879 (2019), https://doi.org/10.1039/c9nr07889d.
[61] F. Shaik, W. Zhang, W. Niu, A generalized method for the synthesis of ligand-free M@SiO2 (M = Ag, Au, Pd, Pt) yolk-shell nanoparticles, Langmuir 33 (2017) 3281–3286, https://doi.org/10.1021/acs.langmuir.7b00141.
[62] X. Qi, X. Li, G. He, Y. Zhu, Y. Diao, H. Lu, Preparation of hollow submicrospheres with ordered porous SiO2 shell and multiple AuPt nanoalloy cores and their high catalytic activity, Chem. Eng. J. 284 (2016) 351–356, https://doi.org/10.1016/j.cej.2015.08.156.